Initiation of Slugs in Horizontal Gas-Liquid Flows

Z. Fan, F. Lusseyran, and T. J. Hanratty
Dept. of Chemical Engineering, University of Illinois, Urbana, IL 61801

Experiments were conducted with air-water flow in a horizontal 0.095-m pipeline at atmospheric pressure to examine the mechanism by which slugs form in a stratified flow. A specially designed entrance box was used to avoid disturbances. In these experiments, at superficial gas velocities less than 3 m/s, the slugs are found to evolve from waves, with a length of about 0.085 m, that are generated by a Jeffreys mechanism. These waves grow in height and eventually double in wavelength by a nonlinear resonance mechanism. Depending on the height of the liquid, the growth can lead to a breaking wave or to a wave that fills the whole pipe cross section. At superficial gas velocities equal to or greater than 4 m/s capillary-gravity waves with a wide range of lengths are generated by a linear Kelvin-Helmholtz mechanism. These rapidly evolve into long waves outside the range of linear instability. If the liquid height is large enough, these waves can form slugs through a nonlinear Kelvin-Helmholtz instability that is aided by wave coalescence.

Introduction

When gas and liquid flow in a pipeline, a slug pattern can be observed, for which aerated blocks of liquid bridge the whole cross section and move intermittently downstream. The manner by which they are formed is of considerable importance in predicting the conditions for initiating the slug pattern and for predicting the frequency of slugging.

Most theoretical work has focused on a Kelvin-Helmholtz mechanism whereby the destabilizing effects of inertia and of gas-phase pressure variations 180 degrees out of phase with the waveheight are larger than the stabilizing effects of gravity and surface tension. Wallis and Dobbins (1973), Lin and Hanratty (1986), and Wu et al. (1987) implemented this notion by examining the stability of a flowing liquid layer to long wavelength disturbances. According to these analyses, slugs evolve directly from infinitesimal waves, which grow to touch the top of the pipe. Kordyban and Ranov (1970), Taitel and Dukler (1976), and Mishima and Ishii (1980) examined the stability of finite amplitude waves. These analyses are not complete in that the origin of the wave is not indicated and information, such as the wavelength and the amplitude of the unstable wave, has to be specified.

Bontozoglou and Hanratty (1990) suggested that slugs could evolve in air/water systems from small-amplitude capillary-gravity waves generated by a Jeffreys sheltering mechanism (an imbalance between energy fed to the wave by gas-phase pressure variations in phase with the wave slope and viscous dissipation). When these waves grow to a certain amplitude, a bifurcation exists whereby they have the possibility of doubling in wavelength. Bontozoglou and Hanratty argued that this bifurcation is the first step in the evolution of these waves to slugs and that the bifurcation is triggered by a subcritical Kelvin-Helmholtz instability. No experimental evidence is available to support this mechanism.

Lin and Hanratty (1987b) reported on visual observations of the initiation of slugs in horizontal 0.051-m and 0.095-m pipelines. The mixer for the air and water at the inlet was a simple tee in which the liquid moved along the run. At gas superficial velocities (defined as the gas volumetric flow divided by the cross section of the empty pipe) below 3 m/s, the first slugs were observed to originate far downstream from the entry. The formation occurred so rapidly that the details could not be documented. With increasing liquid flow rate, the location of the transition was observed to move closer to the inlet. At large enough liquid flow rates, several slugs existed in the pipe at a given time and the slugs originated in the mixing section where the process could not be observed. At superficial gas velocities above 3 m/s, slugs were reported to form as the result of the coalescence of Kelvin-Helmholtz waves.

This study uses both photographic and instrumental methods to obtain information about how slugs evolve. Results are given for air/water flow at atmospheric pressure in a 0.095-m hor-

Z. Fan is currently at Fractionation Research, Stillwater, OK.
F. Lusseyran is visiting scientist from LEMTA-ENSEM, Nancy, France.

izontal pipe at superficial gas velocities less than 10 m/s at different locations along the pipe. No attempt is made to develop a new correlation for the initiation of slugs. The work is a logical extension of previous studies of wave properties at a single location (Andritsos, 1986; Andritsos and Hanratty, 1987a,b; Andritsos et al., 1989).

A specially designed box entry with a converging outlet was fabricated from plexiglas so that, at high liquid rates, the slugs formed within the pipeline and not in the mixer. The time-varying liquid height was measured at a number of locations that were chosen to capture the formation process. The wave pattern at liquid flow rates just below those required to initiate slugging and the details regarding the formation of slugs at the initiation condition were carefully documented.

In the experiments, slugs were found to originate from regular short-wavelength waves at superficial air velocities less than 3 m/s. Downstream, these disturbances evolved into larger-wavelength waves. These grow to a critical height at which they tumble or strike the top of the pipe to form a slug. At superficial velocities greater than 3 m/s, slugs were found to originate from capillary-gravity waves with a range of lengths, which would be predicted to be unstable by a linear Kelvin-Helmholtz analysis. These rapidly evolve into waves with lengths outside the range of linear instability. The growth of these waves to form a slug is enhanced by wave coalescence, such as observed by Lin and Hanratty.

The Experiments

The experiments were conducted in a horizontal pipe that had a diameter of 0.095 m and a length of 24 m. It was contained in a test facility described by Williams (1990). The tank used to contact the gas and liquid at the inlet had a size of 0.45 × 0.43 × 0.37 m. It was connected to the pipeline by a converging pipe with an angle of 5 degrees. This mixing section created less disturbances than a simple tee because of the liquid holdup in the box and because there was a favorable pressure gradient in the converging section.

Three pairs of conductance probes and one pressure transducer were located in the test section in Figure 1. Another pair was located 2.2 m downstream from the test section. The conductance probes, which were used to measure liquid height, consisted of a pair of platinum wires, 0.254 mm in diameter, that were strung across the pipe diameter. A piezoresistive pressure transducer, 4 mm in diameter, was mounted flush with the top wall. Electrical signals from the conductance probes and the pressure transducer were digitized at a rate of 400 points per s. Details regarding the measurement techniques are given in other references (Lin and Hanratty, 1987b; Williams, 1990).

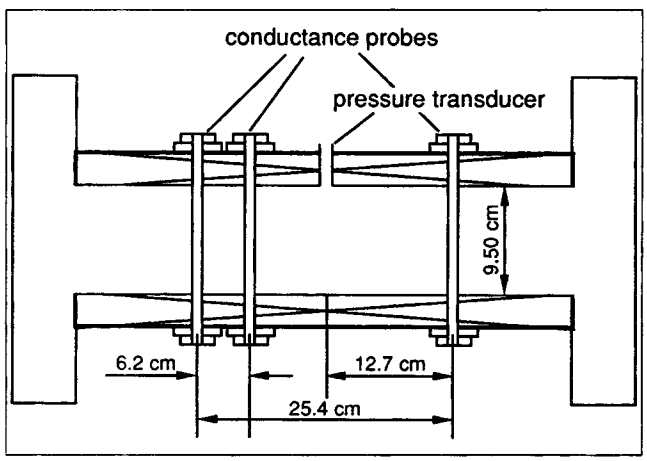

Figure 1. Test section.

Different experiments were done, at the same gas and liquid flow rates, with the test section located at six positions along the pipeline. For each superficial gas velocity, results for three different superficial liquid velocities are reported. One was just below that required to initiate slugs. A second, which was just above the critical velocity, had a frequency of slugging so low that it was possible to obtain information about the wave pattern just before the appearance of a slug in the pipeline. A third was at a liquid velocity that was large enough that at least two slugs could appear in the pipeline at one time.

Initiation of Slug Flow

Visual observations

Consider a fixed gas flow with $u_{SG}<3$ m/s. At low liquid flows, the interface was observed to be smooth or ruffled with very small-wavelength capillary waves. With an increase in liquid flow, long-wavelength waves with small amplitudes appear (of the type in Figure 2a) at a distance downstream from the entry of six pipe diameters. With further increase in liquid flow, short-wavelength waves are superimposed on the long-wavelength waves (see Figure 2b). These short-wavelength waves evolve into symmetric long-wavelength waves of the type in Figure 2c. These can grow in amplitude, as they propagate downstream and eventually reach a critical height at which they tumble to form the asymmetric waves in Figure 3. These breaking waves keep a constant height as they propagate downstream.

At large enough liquid flow rates, the symmetric waves in Figure 2c assume large amplitudes. One of these waves can suddenly jump up to form a liquid bridge across the pipe. This bridge can collapse or grow in length to form a slug. If it forms a slug, there is a sudden increase in the pressure and a calming of the liquid interface behind the slug. When the slug moves out the end of the pipe, one or more slugs form in the pipeline much closer to inlet. As these slugs propagate down the pipe, liquid in the stratified flow is swept up and the liquid level in the whole pipeline drops. This liquid is replenished, and, when the level builds up, the whole cycle is repeated.

For a superficial gas velocity of 1 m/s, Figure 2, the first slug formed at the outlet. This suggests that, at this low gas velocity, there was an effect of fetch. Thus, slugs might have appeared at a lower liquid flow rate if the pipe were longer. For a superficial gas velocity of 2 m/s, the first slug is formed about 3 m away from the outlet so that the critical condition at 2 m/s is believed to be the same as would be observed in longer pipes.

When the gas flow was high ($u_{SG}>3$ m/s), small-amplitude large-wavelength waves of the type in Figure 2a could not be observed. For low u_{SG}, the liquid interface was smooth for low liquid flows. For $u_{SG}>8$ m/s, however, waves were observed at the interface at all liquid heights. These waves develop and reach their maximum height much more rapidly than the waves observed at low gas velocities. They are the "large-amplitude

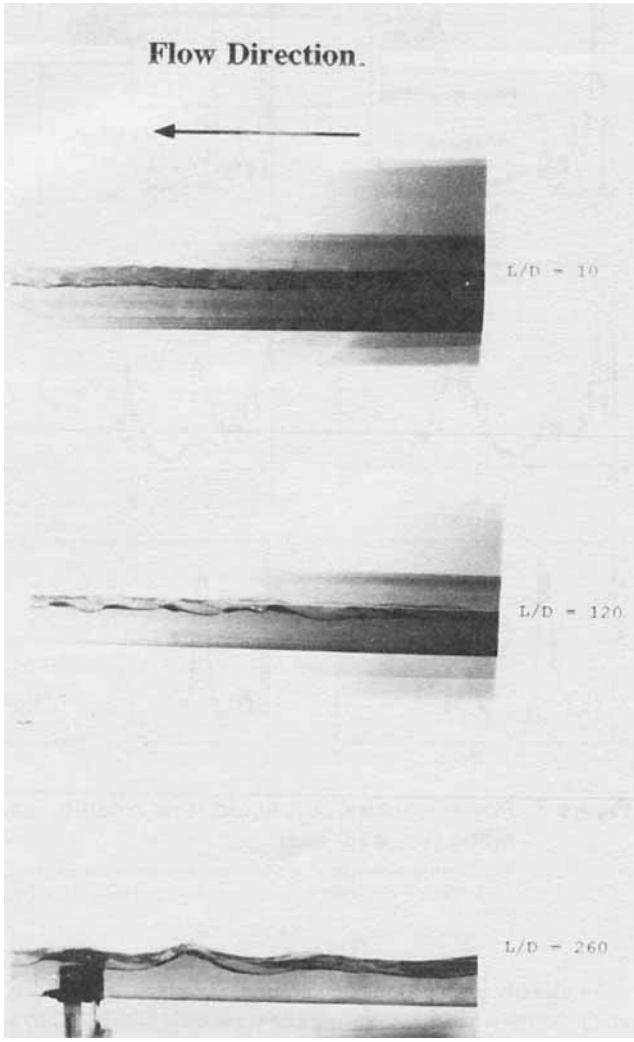

Figure 2. Wave pattern at different locations in the pipeline.

L is the distance from the inlet and *D* is the pipe diameter.

Kelvin-Helmholtz waves" described by Andritsos and Hanratty (1987a). For large enough liquid flows (or liquid heights), the waves can coalesce to form a slug or a pseudoslug. This seems to be the principal mechanism for the formation of slugs at high gas flows, as pointed out by Lin and Hanratty (1987b). However, sometimes single waves are observed, at $u_{SG}>3$ m/s, to grow and reach the top of the pipe. This occurrence is associated with the excessive aeration, so that the wave takes on a foamy appearance.

Conditions for the initiation of slugs

The conditions observed in these experiments for the initiation of slugging are presented in Figure 4 which gives the critical superficial liquid velocity as a function of the superficial gas velocity. (Slug flow exists above and stratified flow, below the points.) For comparison, results obtained by Lin and Hanratty (1986) with a T-mixer at the inlet are also given. It is noted that for a given gas flow, a smaller liquid flow was required to initiate slugging in the experiments of Lin and Hanratty than in our experiments.

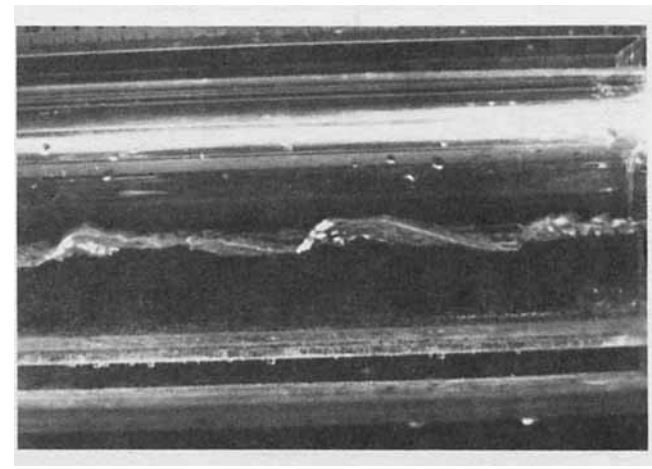

Figure 3. Breaking waves.

Figure 5 shows average dimensionless liquid heights (along the centerline of the pipe) measured for water flows at transition. At low gas flows (u_{SG} = 1–3 m/s) and at low liquid flows, it is noted that $\bar{h}_L/D$ varies, so that the actual gas velocity, $\bar{u}_G = u_{SG}(A/A_G)$, and liquid velocity, $\bar{u}_L = u_{SL}(A/A_L)$, are not constant along the pipeline. The liquid velocity for a given u_{SG} and $\bar{h}_L$ depends on hydraulic gradients, interfacial drag, and wall resistance. The latter is probably associated with the increase in height immediately downstream of the entrance. Differences associated with hydraulic gradients, as well as disturbances introduced at the entry, could account for the influence of the gas-liquid mixer.

The transition results are plotted in Figure 6 as the dimensionless liquid height, $\bar{h}_L/D$, at transition vs. the dimensionless superficial gas velocity, $u_{SG}/(gD)^{1/2}$, and the dimensionless current velocity, $(\bar{u}_G-\bar{u}_L)/gD)^{1/2}$. Here, the average height, $\bar{h}_L$, is defined at the approximate location in the pipeline where slugs are initiated, and $\bar{u}_G$, $\bar{u}_L$ are the actual gas and liquid velocities. The value of $(gD)^{1/2}$ for a 9.53-cm pipe is 0.97 m/s. Consequently, the experiments for $u_{SG}<3$ m/s correspond to current velocities $(\bar{u}_G-\bar{u}_L)$ less than 5 m/s. These results agree with measurements with air-water at atmospheric

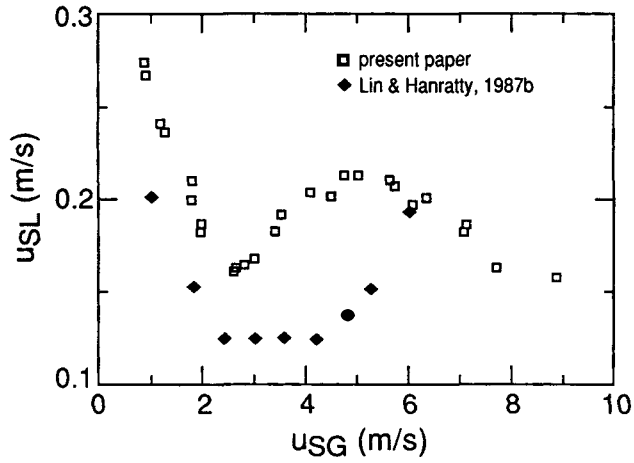

Figure 4. Conditions for the transition from a stratified flow to a slug flow.

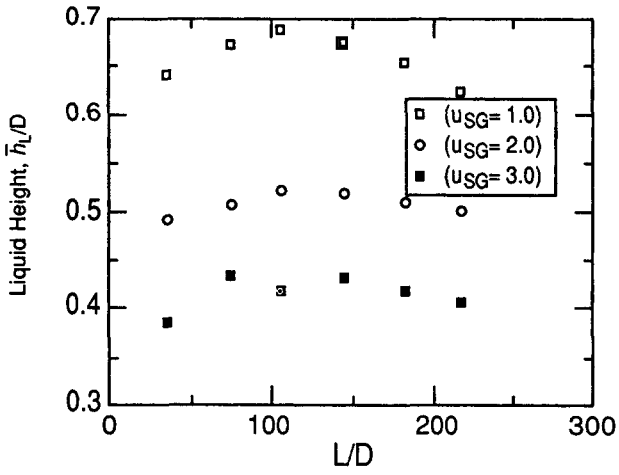

Figure 5. Time-average liquid heights along the pipeline.

pressure reported by Kordyban (1977). They give slightly lower $\bar{h}_L/D$ for transition, but this is expected since the test section used by Kordyban could be too short to eliminate fetch effects.

Figure 6 is presented to correlate the results obtained in this research and to compare them with previous work by Lin and Hanratty. It is not presented as a general prediction. For example, measurements with high-viscosity liquids (Andritsos et al., 1989) show transition lines which are displaced upward from the one in Figure 6. Studies at high pressure also give transition curves different from Figure 6 (Andritsos et al., 1992; Hanratty, 1991). Somewhat better agreement for moderate changes in pressure would be obtained by multiplying the abscissa by $\sqrt{\rho_G/\rho_L}$. However, as pointed out by Hanratty (1991), this might not be valid for very large gas densities, where a different mechanism could be operative.

It is noted that the measurements of the critical $\bar{h}_L/D$ in the experiments of Lin and Hanratty and the present experiments are much closer than the measurements of the superficial liquid velocities. A comparison of Figures 4 and 6 suggests that the differences in the critical u_{SL} are associated mainly with differences in the actual liquid velocity at transition.

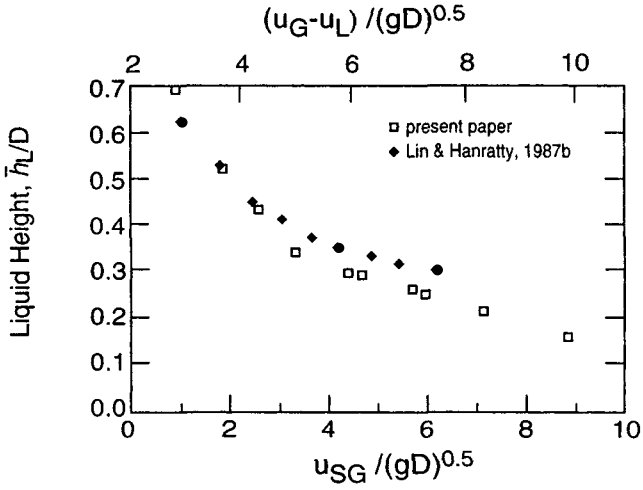

Figure 6. Liquid heights measured at the transition from stratified flow to slug flow in a 9.53-cm pipe at atmospheric pressure.

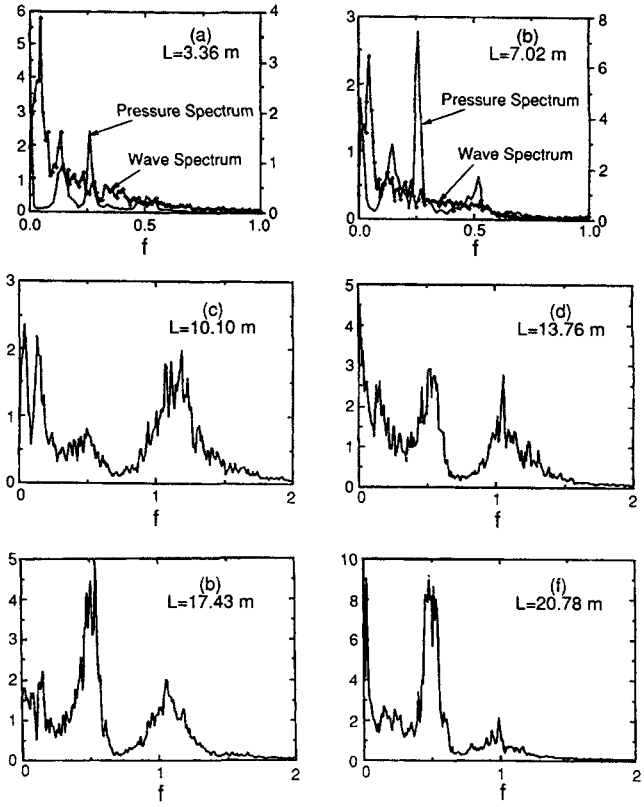

Figure 7. Power spectra of a liquid flow close to transition (u_{SG} = 1.0 m/s).

The dimensionless spectra density functions are multiplied by 10^6. Wave spectra are on the left ordinate. Pressure spectra are on the right.

As already pointed out by Lin and Hanratty, Figure 6 is a much better way of presenting the transition results from the viewpoint of theoretical interpretation. The dependency of the critical superficial liquid velocity on equipment design in Figure 4 indicates that the critical $\bar{h}_L/D$ is not very sensitive to changes in u_{SL} for the conditions existing in these experiments. The conclusion drawn is that slight changes in the critical $\bar{h}_L/D$ caused by equipment design translates into large changes in the critical liquid flow rate.

As discussed earlier, the details of what happens after the initiation of slugging depends on the outlet design, as well as on the inlet design. However, the same length of piping and the same type outlet were used in the present experiments and the experiments of Lin. Consequently, observed differences are probably associated with changes in the inlet design. The outlet design can influence hydraulic gradients in the pipeline, but a more important effect would be the pipe length. If a much longer pipe were used, the distance from the initiation point and the discharge point would be larger so that, when the slug discharges from the pipe, the liquid in the initiation region would build to larger heights than were observed in this research. The critical conditions in Figure 6 are for short enough pipelines that the slug discharge from the outlet is not affecting the initiation of the slugging cycle described earlier.

Wave properties prior to slug initiation for $u_{SG} < 3$ m/s

Measurements of dimensionless wave spectra at a liquid flow

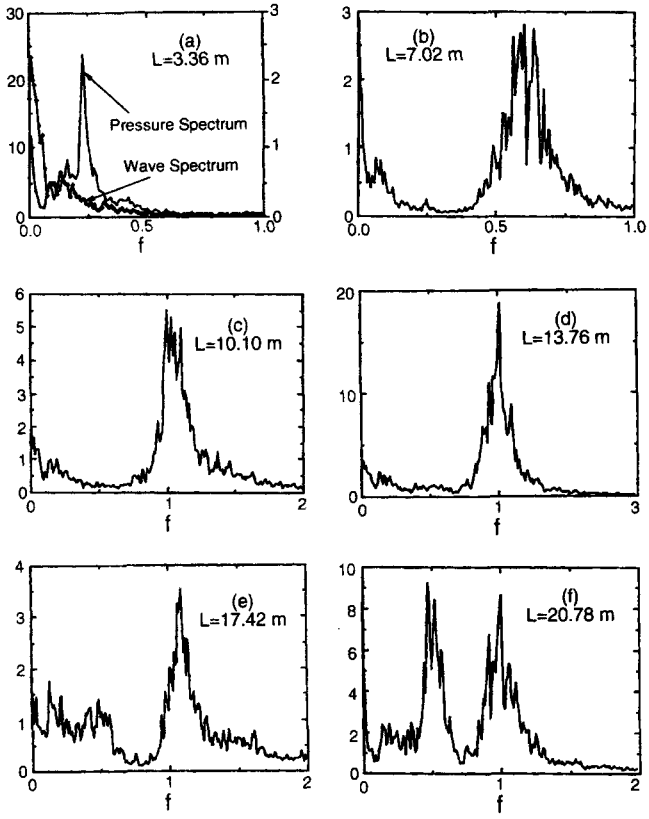

Figure 8. Power spectra of a liquid flow close to transition (u_{SG} = 2.0 m/s).

The spectral density functions are multiplied by 10^6. Wave spectra are on the left ordinate. Pressure spectra are on the right.

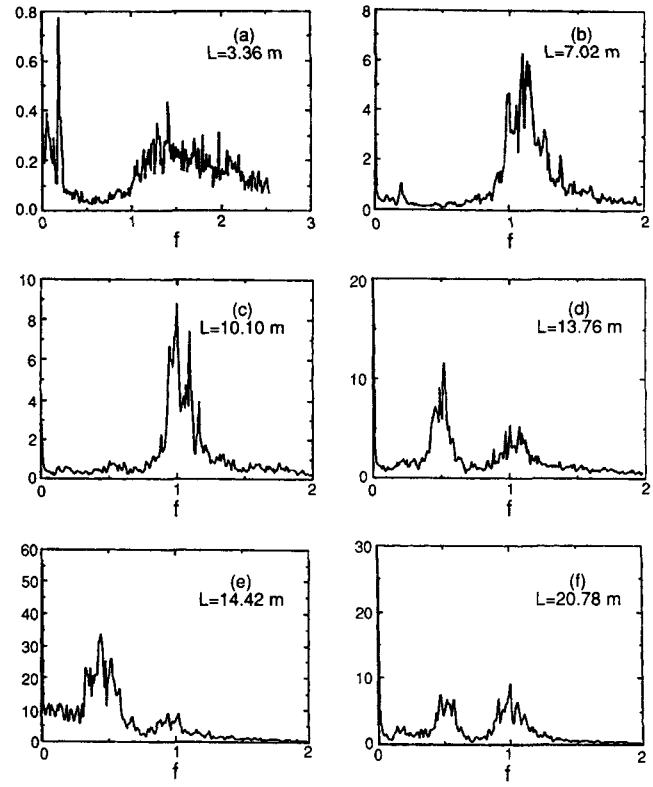

Figure 9. Power spectra for waves at a liquid flow close to the transition (u_{SG} = 3.0 m/s).

The spectral density functions are multiplied by 10^6.

rate just below that required to initiate slugs are given in Figures 7-9. The total dimensionless energies associated with these spectra are given in Figure 10. Unless otherwise designated, all of the variables are made dimensionless with the pipe diameter, D, and the acceleration of gravity, g. Thus, the frequency, f, in these plots has been made dimensionless with $(gD)^{1/2}$.

Figure 7 gives the spectral density function of the liquid height for u_{SG} = 0.95-1.1 m/s. The measurements at L = 3.36 m and at L = 7.02 m would correspond to conditions between those depicted in Figures 2a and 2b. A principal peak occurs at a low dimensionless frequency of about f = 0.06 (0.6 cps) and a secondary peak at f = 0.12 (1.2 cps). These correspond to the long-wavelength wave in Figure 3a. Two peaks at f = 0.12 and f = 0.25 are also observed in the spectral density function for the pressure fluctuations. The measurement of the wave spectrum in Figure 7c corresponds roughly to the wave pattern in Figure 2b. The peaks at f = 0.06 and f = 0.12 are still evident, but a peak with a large amount of energy appears at f = 1.2 (12 cps). This corresponds to the short-wavelength waves in Figure 2b. A peak with much smaller energy is also observed at f = 0.5 (5 cps) for L = 10.10 m. It is noted that this peak grows with distance downstream and that the higher frequency peak shifts from f = 1.2 to f = 1.0. At L = 20.78 m, the f = 0.5 wave is dominant. It appears that this wave can be sustained from energy fed by the air flow to the liquid. In a long enough pipe, it could grow until it breaks or reaches the top of the pipe.

Wave height spectra for u_{SG} = 2 m/s and 3 m/s in Figures 8 and 9 show qualitatively the same behavior as for 1 m/s in that the wave pattern that evolves downstream is characterized by two spectral peaks at f = 0.5 and f = 1.0. These data show that high-frequency waves develop closer to the inlet for the higher gas velocities. The peak close to f = 1.0 appears first. This suggests that these waves are generated directly by the air flow and that the f = 0.5 waves evolve from them. For u_{SG} = 2 m/s, between L = 13.76 m and L = 17.42 m, there is a large transfer of energy from the f = 1 wave to low-frequency waves in the range of f = 0 to 0.5 and a slight decrease in the total power. Between L = 17.42 m and L = 20.78 m a wave with f = 0.5 emerges, and there is a slight increase in the total power.

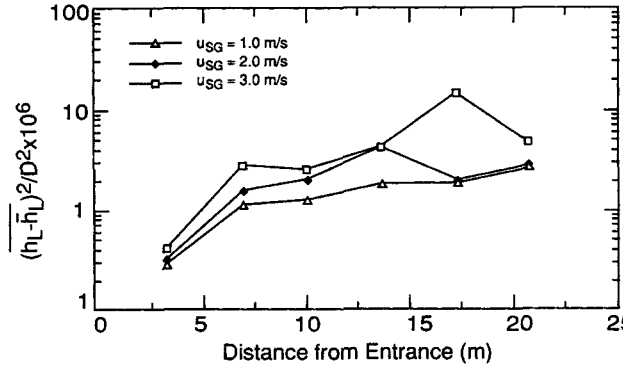

Figure 10. Total power of the wave spectra.

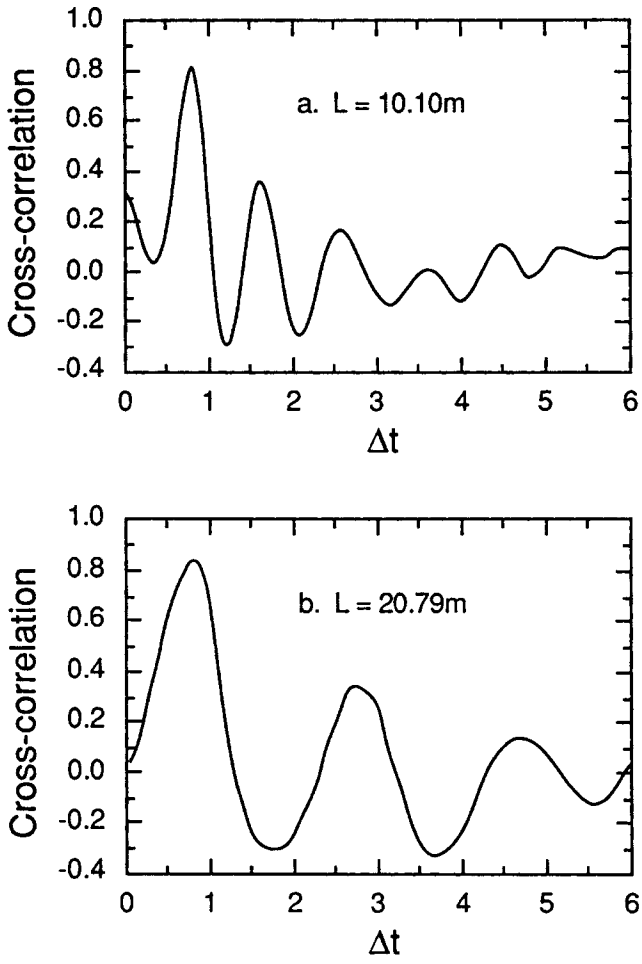

Figure 11. Cross correlations of wave displacement.

The increase in the energy of the $f=1$ wave between $L=17.42$ m and $L=20.78$ m could be associated with a transfer of energy from the air flow to this wave and/or a transfer of energy from the $f=0.5$ wave. For $u_{SG}=3$ m/s, a broad spectrum of high-frequency waves develops close to the entry ($L=3.36$ m). This narrows down to a spectrum with a relatively sharp peak at $f=1.0$. At $L=13.76$ cm, a peak at $f=0.5$ is seen to develop. For this particular velocity, the liquid height is smaller than for $u_{SG}=1.0$ and 2.0 m/s. It is well known (Cohen and Hanratty, 1965) that if the ratio of $\lambda/\bar{h}_L$ is large enough, viscous dissipation is greatly enhanced. Consequently, the decrease in the height of the $f=0.5$ peak between $L=17.42$ m and $L=20.78$ m can be explained if viscous dissipation is large enough that a $f=0.5$ wave cannot be sustained by the air flow. This behavior is also illustrated in Figure 10, which shows that the total power of the wave decreases significantly between $L=17.42$ m and $L=20.78$ m for $u_{SG}=3$ m/s.

The characteristics of wave bifurcation are that the wavelength doubles, the wave frequency halves, and the wave velocity is constant. Cross correlation functions of liquid height fluctuations, obtained with two liquid height probes separated by a distance of 6.2 cm, are shown in Figure 11 for a superficial gas velocity of 1 m/s. Figure 11b at $L=20.79$ m, corresponds to the spectrum in Figure 7f, which suggests a wave pattern dominated by a wave with $f=0.5$ (5.0 cps). The cross correlation is consistent with this in that it shows peaks and troughs separated by dimensionless time delays at $\Delta t=2$. The first peak occurs at a dimensionless time delay of $\Delta t=0.75$. This gives a dimensionless wave velocity $[C/(g_D)^{1/2}]$ of 0.87 (0.81 m/s) and a dimensionless wavelength $\lambda/D=1.74$ (17 cm), since $\lambda=C/f$. The cross correlation at $L=10.10$ m in Figure 11a corresponds to the spectrum in Figure 7c, which is dominated by waves with a dimensionless frequency of 1.1. It is noted that the peaks and troughs in the cross correlation are separated by $\Delta t=1$, corresponding to the smaller-frequency wave. From the first peak, a dimensionless wave velocity of 0.87 (0.81 m/s) and a dimensionless wavelength of $\lambda/D=0.87$ (8.5 cm) are obtained.

Table 1 summarizes wave properties measured in this way for $u_{SG}/(gD)^{1/2}=1, 2, 3$. The dimensionless wave velocities of the two wave components are given in terms of $(C-\bar{u}_L)$ rather than of C. The measured wavelengths, equal to C/f, are given in the 7th and 8th columns, where f was obtained from the spectral measurements. Wave velocities calculated from these two measured wavelengths with linear theory for a two-dimensional flow are given in columns 9 and 10. To apply linear theory to a pipe flow, the effective heights of the liquid and gas were taken as A_L/S_i and A_G/S_i, where A_L and A_G are the areas of the liquid and gas, and S_i is the length of the interface. It is noted that the measured wave velocity (column 6) is approximately equal to the wave velocity calculated from linear theory for the large-wavelength wave, but is significantly larger than the calculation for the small-wavelength wave. The difference between the measured wave velocity for the λ_1 waves and the wave velocity calculated by linear theory indicates that the bifurcation follows a nonlinear mechanism, as will be discussed later.

Of particular interest is the observation that the wave which is the precursor of the formation of a slug has the same wavelength (8.5 cm), wave velocity and frequency over the range of gas velocities studied, $u_{SG}=1$-3 m/s. This suggests that these wave characteristics scale with D and $(gD)^{1/2}$ for horizontal air-water flows. Experiments in a pipe with a different diameter would be most useful.

Wave properties prior to slug formation for $u_{SG}>3$ m/s

Wave spectra for $u_{SG}>3$ m/s are shown in Figures 12 and 13. Median frequencies characterizing these spectra are given

Table 1. Wave Properties for $u_{SG} \leq 3$ m/s

$u_{SG}/\sqrt{gD}$	$u_{SL}/\sqrt{gD}$	$\bar{u}_G/\sqrt{gD}$	$\bar{u}_L/\sqrt{gD}$	$\bar{h}_L/D$	$[(C-\bar{u}_L)/\sqrt{gD}]_{EX}$	λ_1/D	λ_2/D	$[(C-\bar{u}_L)/\sqrt{gD}]_{linear}$ for λ_1	$[(C-\bar{u}_L)/\sqrt{gD}]_{linear}$ for λ_2
1.0	0.29	4.4	0.38	0.69	0.49	0.89	1.78	0.40	0.52
2.0	0.21	4.8	0.40	0.52	0.48	0.88	1.76	0.39	0.50
3.0	0.17	5.0	0.42	0.42	0.49	0.90	1.81	0.38	0.49

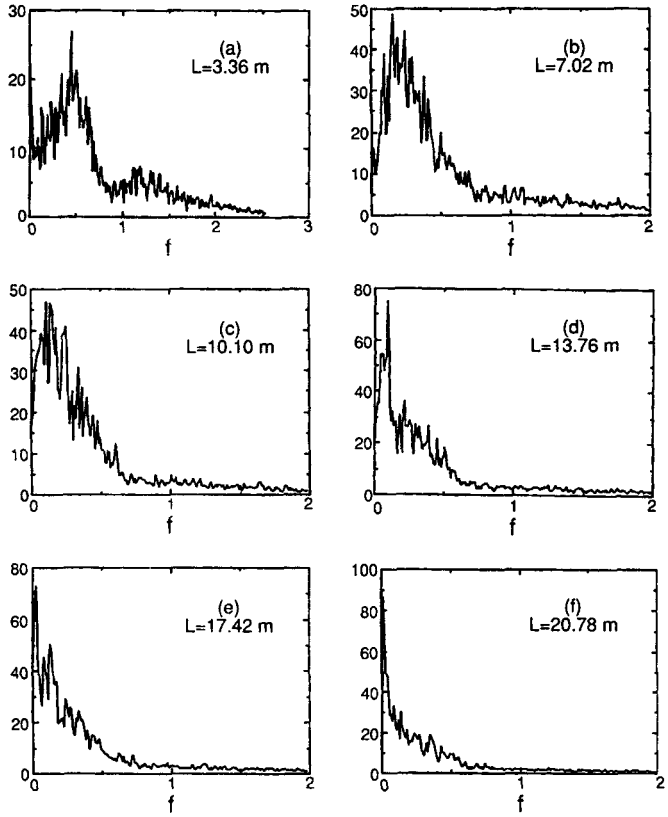

Figure 12. Power spectra of waves for $u_{SG} = 4.0$ m/s.

The dimensionless spectral density function on the ordinates is multiplied by 10^6.

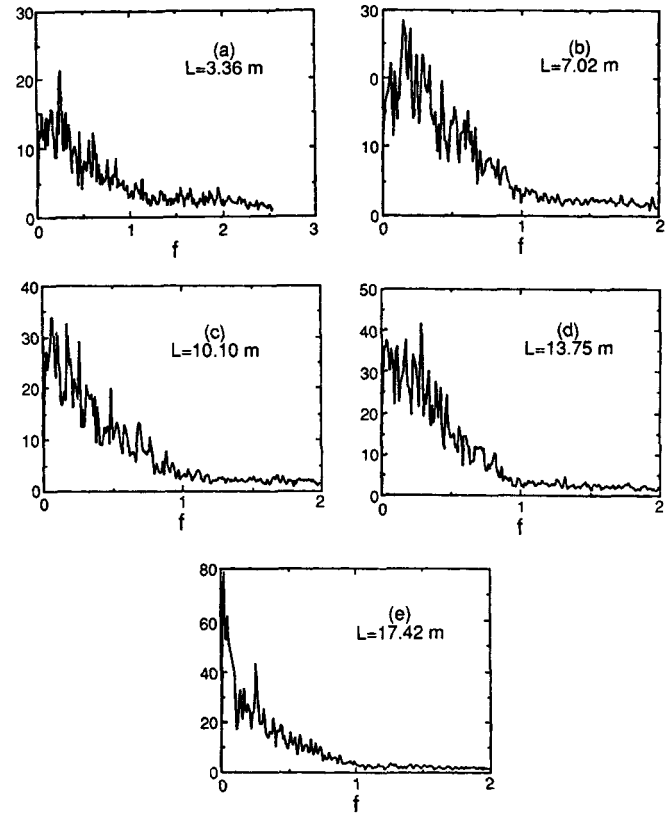

Figure 13. Power spectra of waves of $u_{SG} = 6.0$ m/s.

The dimensionless spectral density functions on the ordinates are multiplied by 10^6.

in Figure 14. Typical wave patterns are presented in Figures 15, 16 and 17.

Figure 12 shows results for $u_{SG} = 4$ m/s. Close to the inlet ($L = 3.36$ m), a peak at $f = 1.2$ is observed, but the dominant feature is a broad spectrum of low-frequency, long-wavelength waves.

For $L \geq 7.02$, a peak occurs at $f \cong 0.2$ to 0.4. As seen from the tracing in Figure 15, this represents groups of short-wavelength waves. The tracing at $L = 13.76$ m (Figure 16) shows these groups of waves to evolve into a pattern of large-amplitude roll waves similar to what was observed in a rectangular channel by Hanratty and Engen (1957).

It is noted also from the spectra that a very long-wavelength wave ($f \approx 0$) starts to develop for $L \geq 7.02$ m. There are hints of this in the tracings at $L = 7.02$ m and at $L = 20.79$ m (Figure 17). Longer time records, however, clearly show a modulation of the wave pattern with a very low-frequency disturbance.

Spectra for $u_{SG} = 6$ m/s are given in Figure 13. These show the same behavior as for $u_{SG} = 4$ m/s, except that the peak at $f = 1.2$ is not evident at $L = 3.36$ and the wave frequencies are higher.

Slug Flow Close to Transition for $u_{SG} \leq 3$ m/s

This section focuses on the initiation of slugs at liquid flows slightly above the critical values shown in Figures 4 and 8 at $u_{SG} \leq 3$ m/s. Its purpose is to provide a better understanding of the evolution of slugs from an unstable wave pattern. The experiments were performed by adjusting the liquid flow rate so that slug formation would occur close to the location of the test section in Figure 1. When the superficial gas velocity is kept constant, at a value less than or equal to 3 m/s, slugs first appear close to the outlet of the pipeline. With further increases in liquid flow, the frequency of slugging increases and the position at which slugs are initiated moves toward the entrance of the pipeline.

When the liquid flow rate is at or slightly above the critical

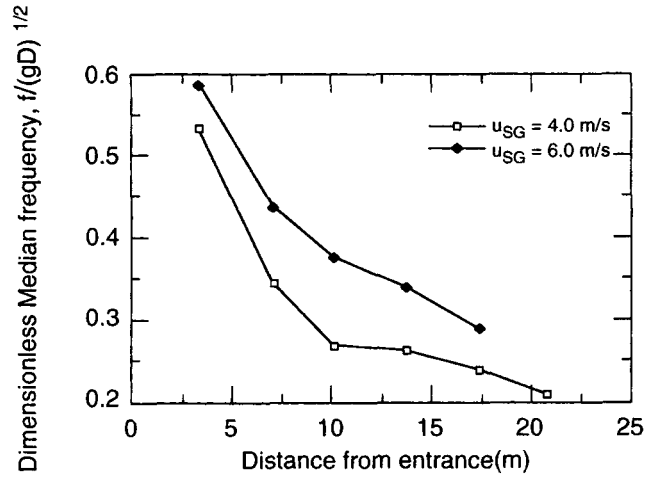

Figure 14. Change of the median frequency of the waves with distance from the entrance.

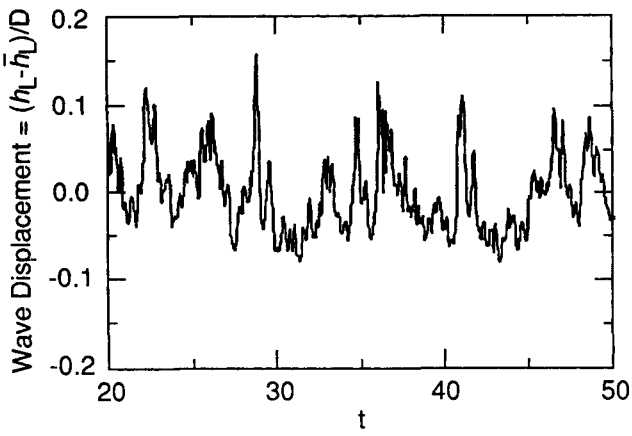

Figure 15. Wave displacement for $u_{SG}=4.0$ m/s, $L=7.02$ m.

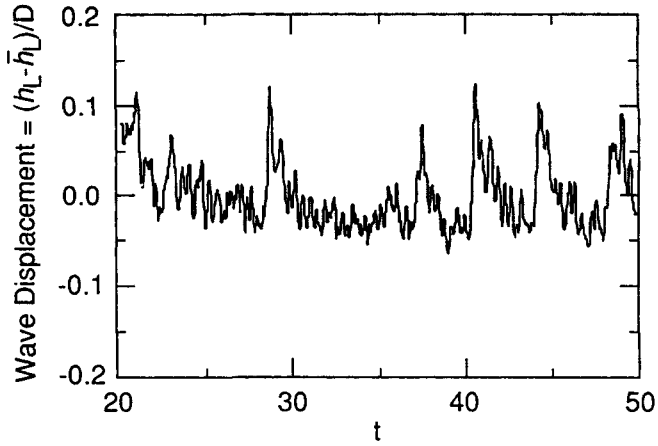

Figure 17. Wave displacement for $u_{SG}=4.0$ m/s, $L=20.79$ m.

value, only one slug will exist in the pipeline and the wave structure in front of this slug is the same as described later. Figure 18 shows liquid holdup, $\bar{h}_L/D$, as a function of time measured at $L=4.5$ m for $u_{SG}=1.48$ m/s and $u_{SL}=0.33$ m/s. The liquid slug in this figure has a velocity of 2.19 m/s and a length of 0.46 m. Because of aeration, the holdup $\bar{h}_L/D$ is not equal to unity. The liquid height of $\bar{h}_L/D=0.58$ represents, approximately, the stratified flow that existed when the slug was initiated. As the slug propagates downstream, it picks up liquid at its front and sheds it at a lower rate at its rear. The slug thus is growing in size.

A spectrum obtained by taking a Fourier transform of the liquid height fluctuations before the arrival of the slug shows two peaks. One is at a dimensionless frequency of $f=1.0$ and the other is at $f=0.6$. There is also another peak at very low frequency, $f\approx 0$. There is a similarity with the spectra in Figure 7 for $L=10.10$ cm and $L=13.76$ m when the superficial gas velocity is around 1.0 m/s.

When the slug in Figure 18 moved out of the system, the liquid in the pipeline was at a reduced level. It had to build up to a critical value before another slug appeared. This process was documented rather carefully for a $u_{SG}=2.34$ m/s and $u_{SL}=0.251$ m/s. Figure 4 shows that this is at a liquid flow which is significantly higher than the critical. As a consequence, slugs were initiated in the pipeline at $L<3.5$ m, as well as downstream.

Figure 19 shows a tracing of the liquid level at $L=3.5$ m. The slug in the figure is moving at a velocity of 2.9 m/s and has a length of 0.44 m. It is noted that the height of the stratified flow on which the slug was initiated is roughly equal to the critical height $\bar{h}_L/D=0.48$ in Figure 6; it is not the height that a stratified flow would reach at this gas and liquid flow under equilibrium conditions. An examination of the liquid level over a period of time showed an increase from the height of $\bar{h}_L/D=0.14$ to the height of 0.48. Initially, the interface is relatively smooth. As the liquid level builds up, small-wavelength waves appear. Sometime later, these waves suddenly disappear over the whole length of the pipe. This observation coincided with a sudden increase in the gas-phase pressure and the appearance of a slug downstream. This calming could be associated with a sudden transient decrease in the gas velocity, caused by the blocking of the pipe cross section by the slug. Several seconds later, waves with a length of 4 to 7 cm suddenly appeared. This is coincident with the exiting of the slug from the pipe and a sudden decrease in pressure. It is presumed that waves appear because of a sudden transient increase in the gas velocity. The tracing in Figure 19 shows a calm surface followed

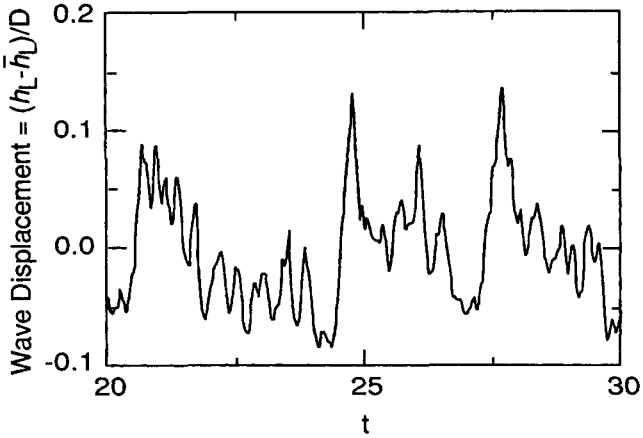

Figure 16. Wave displacement for $u_{SG}=4.0$ m/s, $L=13.76$ m.

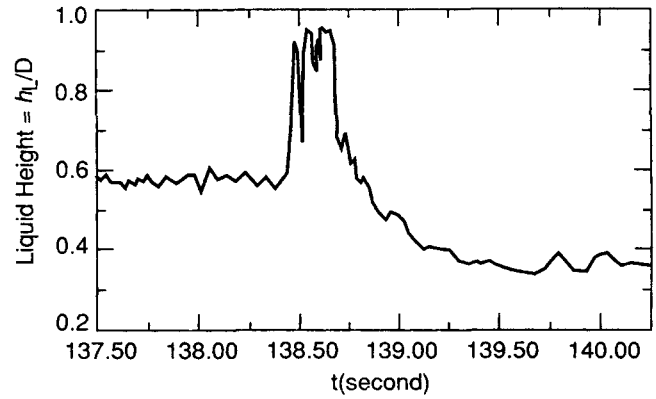

Figure 18. A slug initiated 17 m away from the entrance ($u_{SG}=1.3$ m/s).

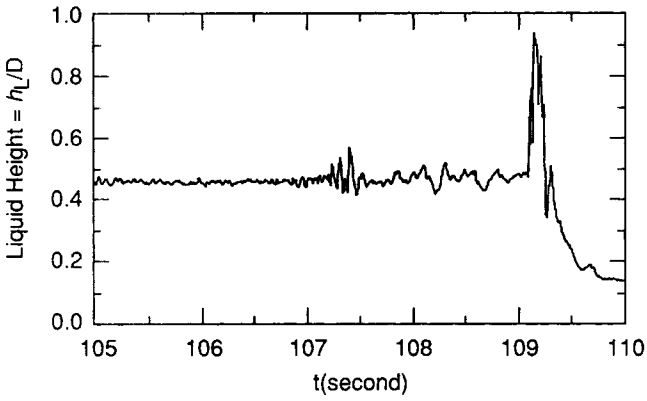

Figure 19. A slug initiated 3.5 m from the entrance at $u_{SG}=2.34$ m/s.

by relatively large-amplitude waves. A frequency spectrum obtained by doing a Fourier transform of the wave record in front of the slug in Figure 19 for t from 107 to 109 s shows peaks at $f\approx 1$ and at $f\approx 0.5$.

Discussion of Results for $u_{SG}\leq 3$ m/s

The results for $u_{SG}\leq 3$ m/s clearly show the appearance of a long-wavelength instability close to the pipe entry for superficial liquid velocities just below those in Figure 4. These waves are quite likely the result of the long-wavelength Kelvin-Helmholtz instability described by Lin and Hanratty (1987) and Wu et al. (1987); they have the possibility of developing into a slug. However, for the experiments described here, smaller-wavelength gravity waves also appear, and these dominate the interfacial pattern. The dominant small-wavelength wave that emerges close to the entrance has the possibilities that it grows to a large enough height that it tumbles, that it reaches the top wall or that it passes energy to other wave harmonics. In all the cases studied, the height of this wave was limited because it passed energy to a wave with twice its wavelength.

The process for this doubling in wavelength appears to be qualitatively the same as the bifurcation discussed by Chen and Saffman (1979, 1980). This theory considers two waves with wavelengths of λ_1 and $\lambda_2=2\lambda_1$, which are predicted to have different wave velocities by linear theory. Because of the influence of wave height, these two waves can assume the same velocity so that a resonant interaction and, therefore, a rapid transfer of energy is possible. Table 1 shows this behavior. The wave velocity of the finite amplitude $f=1.0$ wave is larger than predicted by linear theory and approximately equal the wave velocity for a $f=0.5$ wave predicted by linear theory.

The growth of the λ_2 wave can be limited either because it decays as a result of viscous effects or it reaches a maximum height at which it tumbles or breaks. An enhanced dissipation of the λ_2 wave can occur since the ratio of $\lambda_2/\bar{h}_L$ could be large enough that the solid boundaries greatly increase the dissipation of wave energy (Cohen and Hanratty, 1965; Hanratty, 1983). Thus, in the case considered in Figure 7 for $\bar{h}_L/D=0.69$, $u_{SG}=1.0$ m/s, the dimensionless wave number corresponding to λ_2 is $2\pi\bar{h}_L/\lambda_2\cong 2.4$, and the λ_2 wave continues to grow. However, Figure 9 presents results with $\bar{h}_L/D=0.42$, $u_{SG}=3$ m/s for which $2\pi\bar{h}_L/\lambda_2\cong 1.5$. Here, it appears that viscous dissipation limits growth of the λ_2 wave.

Some understanding of the possibility for the λ_2 wave to grow until it reaches a limiting height can be obtained by considering results of Banner and Phillips (1974). They suggest that wave breaking occurs when the velocity of the liquid at the crest (or very close to it) is equal to the wave velocity. This notion is applied here to stratified flow in a pipeline. Only the bifurcated long wave is considered. The amplitude of short waves, which override the long wave, should be very small due to drift effects (Phillips and Banner, 1974). The analysis is carried out in a reference frame moving at the phase speed C.

The use of the Bernoulli equation at the crest and at the average height of the liquid gives:

$$\eta_C=\frac{1}{g\rho_L}(P_{iL1}-P_{iLC})+\frac{1}{2g}[(u_{iL1}-C)^2-(u_{iLC}-C)^2] \quad (1)$$

where η_C is the displacement of the wave crest, P_{iL1} and P_{iLC} are the pressures at the liquid surface, and u_{iL1} and u_{iLC} are the velocities of liquid particles in the wave surface at the average height, point 1, and at the crest, point C. For surface waves without liquid current, Lamb (1953) has proven that the orbital velocities of liquid particles on the surface at the average liquid height are zero. In a similar way, it can also be proven in the case discussed here that the orbital velocity of liquid particles at the average height is equal to the liquid current velocity, $\bar{u}_L$. Furthermore, from the agruments of Banner and Phillips, the velocity $u_{iLC}\cong C$ when the waves start to break. Therefore, the maximum liquid displacement, η_M is approximated as:

$$\eta_M=\frac{1}{g\rho_L}(P_{iL1}-P_{iLC})+\frac{1}{2g}(C-\bar{u}_L)^2 \quad (2)$$

At the wave surface, $P_{iL}=P_{iG}$ since capillarity is not important. The pressure change in Eqs. 1 and 2 can, therefore, be obtained from an analysis of the gas phase.

Assume a two-dimensional ideal flow for the gas phase, so that the potential function and the stream function can be approximated by the following equations for symmetric waves in a frame of reference moving with velocity C:

$$\frac{\Phi}{u_G-C}=-x-\gamma\cosh k(\bar{h}_G-y)\sin(kx+\xi), \quad (3)$$

$$\frac{\Psi}{u_G-C}=-y+\gamma\sinh k(\bar{h}_G-y)\cos(kx+\xi) \quad (4)$$

where γ is a constant, ξ is the phase, $\bar{h}_G$ is the average height of the gas space, and $\bar{u}_G$ is the average gas velocity. At the wave surface, $\Psi=0$. Therefore, the wave profile is:

$$\eta=\gamma\sinh k(\bar{h}_G-\eta)\cos(kx+\xi), \quad (5)$$

where ξ is taken as $-\pi/2$.

The pressure in the gas phase is then given as:

$$\frac{P_G}{\rho_G}=\text{const}-g\eta-\frac{1}{2}\left[\left(\frac{\partial\Phi}{\partial x}\right)^2+\left(\frac{\partial\Phi}{\partial y}\right)^2\right] \quad (6)$$

From Eq. 3,

$$\frac{\partial \Phi}{\partial x} = -(\bar{u}_G - C)\left[1 + \gamma k \cosh k(\bar{h}_G - y) \cos\left(kx - \frac{\pi}{2}\right)\right] \quad (7)$$

$$\frac{\partial \Phi}{\partial y} = (\bar{u}_G - C)k\gamma \sinh k(\bar{h}_G - y) \sin\left(kx - \frac{\pi}{2}\right). \quad (8)$$

At position 1 on the wave surface, $kx = 0$ and $y = 0$ so that:

$$\left(\frac{\partial \Phi}{\partial x}\right)_1 = -(\bar{u}_G - C), \quad (9)$$

$$\left(\frac{\partial \Phi}{\partial y}\right)_1 = -(\bar{u}_G - C)k\gamma \sinh k(\bar{h}_G), \quad (10)$$

At position C (the wave crest), $kx = \pi/2$ and $y = \eta_C$:

$$\left(\frac{\partial \Phi}{\partial x}\right)_C = -(\bar{u}_G - C)[1 + \gamma k \cosh k(\bar{h}_G - \eta_C)], \quad (11)$$

$$\left(\frac{\partial \Phi}{\partial y}\right)_C = 0, \quad (12)$$

Constant γ can be expressed in terms of the wave height, η_C, as:

$$\gamma = \frac{\eta_C}{\sinh k(\bar{h}_G - \eta_C)} \quad (13)$$

By substituting Eqs. 9, 10, 11, 12 and 13 into Eq. 6, the pressure change in the gas phase on wave surface from position 1 to C is obtained as:

$$\frac{P_{G1} - P_{GC}}{\rho_G(\bar{u}_G - C)^2} = \frac{g\eta_C}{(\bar{u}_G - C)^2} + \eta_C k \coth k(\bar{h}_G - \eta_C) + \frac{1}{2}k^2\eta_C^2 \coth^2 k(\bar{h}_G - \eta_C) - \frac{1}{2}k^2\eta_C^2 \frac{\sinh^2 k\bar{h}_G}{\sinh^2 k(\bar{h}_G - \eta_C)} \quad (14)$$

By substituting Eq. 14 into Eq. 2, an equation for the maximum wave height is obtained:

$$\eta_M = \frac{\rho_G(\bar{u}_G - C)^2}{g\rho_L}\left[k\eta_M \coth k(\bar{h}_G - \eta_M) + \frac{1}{2}(k\eta_M)^2 \coth^2 k(\bar{h}_G - \eta_M) - \frac{1}{2}(k\eta_M)^2 \frac{\sinh^2 k\bar{h}_G}{\sinh^2 k(\bar{h}_G - \eta_M)}\right] + \frac{1}{2g}(C - \bar{u}_L)^2 \quad (15)$$

The analysis for P_G given above is similar to what was presented by Kordyban and Ranov (1970) and by Mishima and Ishii (1980). It is approximate since the waveform assumed does not allow for the pressure condition to be satisfied along the whole interface and the system considered is two-dimensional. Its application to a pipe flow is implemented by taking $\bar{h}_L$ as equal to $\bar{A}_L/\bar{S}_i$, where A_L is the area of the liquid and S_i is the length of the interface.

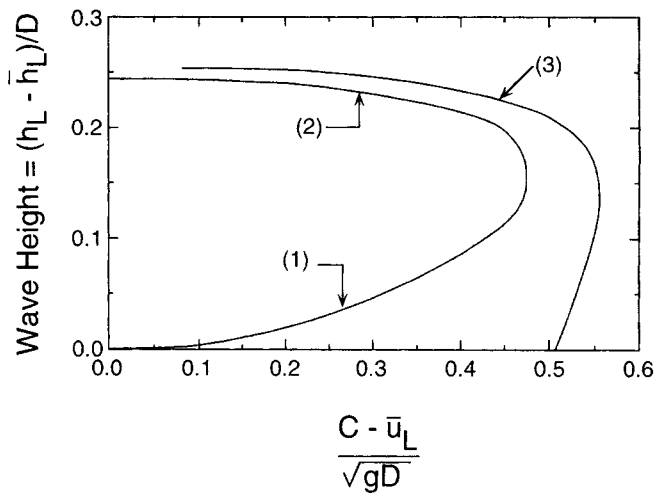

Figure 20. Maximum heights with lower branch (1) and upper branch (2), calculated for $u_{SG} = 2.0$ m/s, $\bar{h}_L/D = 0.5$.

Curve 3 are wave velocities calculated by theory from Kordyban and Ranov for the same conditions.

Figure 20 presents a plot of Eq. 15 for $u_{SG}/(gD)^{1/2} = 2.0$, $2\pi D/\lambda = 2\pi/1.74$, and $\bar{h}_L/D = 0.50$. The wave height, η, is made dimensionless with respect to D and the wave velocity, relative to $(gD)^{1/2}$. The two branches of the solution of Eq. 15 are designated by curves 1 and 2. The relative gas velocity, $(\bar{u}_G - C)$, is increasing as one proceeds along the lower branch on to the upper branch. The lower branch for very small $(C - \bar{u}_L)$ is approximated by the result for zero $(\bar{u}_G - C)$,

$$\eta_M = \frac{1}{2g}(C - \bar{u}_L)^2 \quad (16)$$

In this range, the destabilizing effect of inertia $[(C - \bar{u}_L)^2]$ is counterbalanced by the stabilizing effect of gravity $[g\eta_M]$. As the wave height increases, the gas velocity above the crest increases and the pressure in the gas decreases to provide an additional destabilizing effect. Consequently, a smaller $(C - \bar{u}_L)$ than indicated by Eq. 16 is needed. The influence of gas-phase pressure variations become more important along the upper branch and $(C - \bar{u}_L) = 0$ represents a static instability for which gas-phase suction at the crest equals the restoring force of gravity.

Figure 20 shows two possibilities for the limiting height of a growing wave. The wave is assumed to break, if the height, as it increases, follows a trajectory that intersects the bottom branch. However, if the trajectory bypasses curves 1 and 2, the wave has the possibility of increasing until a Kelvin-Helmholtz instability causes it to jump suddenly to hit the top wall.

Curve 3 in Figure 20 shows wave velocities as a function of wave height, calculated with the approximate relation developed by Kordyban and Ranov, using the same conditions for which curves 1 and 2 were calculated. It is noted that for this case the limiting wave height would never be reached so the liquid would be predicted to reach the top wall, if viscous dissipation were small enough to allow the wave to grow. It is of interest to note the conditions used to calculate this curve are close to ones for which slug formation was observed.

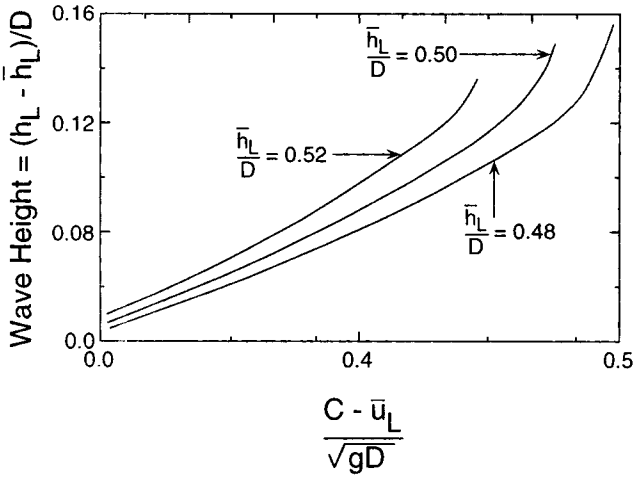

Figure 21. Influence of the average liquid height on the maximum wave height calculated at $u_{SG} = 2.0$ m/s.

The calculated curves in Figure 20 are very sensitive to changes in $\bar{h}_L/D$ and u_{SG} but are not too sensitive to the choice of wave number (at least in the range characterizing the longer waves observed in the experiments). Figure 21 shows the effect of small changes of $\bar{h}_L/D$ on the calculated maximum wave height, for a superficial gas velocity of 2.0 m/s and a dimensionless wave number of $2\pi/1.74$. These calculations suggest that a small change in the height of the liquid can open the possibility of a wave growing to a height such that a nonlinear Kelvin-Helmholtz instability forms a slug. Figure 21 suggests that, at $u_{SG} = 2.0$ m/s, slugs could be formed from the observed long-wavelength waves at $\bar{h}_L/D \cong 0.48$. However, this will occur only if viscous dissipation is not larger than energy supplied to the waves by the gas phase and if the pipe is long enough for the wave to grow to its full height. Considering these factors and the roughness of the calculations, the estimate of a critical $\bar{h}_L/D$ is in satisfactory agreement with the measured value of $\bar{h}_L/D \cong 0.52$ in Figure 6.

Observations of the formation of slugs, as captured on videotape, for $u_{SG} \leq 3$ m/s are also consistent with the analysis given above. Here, it is found that after the waves reach a certain height the liquid around the crest of the wave will suddenly decrease in velocity (or even appear to freeze) and jump vertically upward.

The calculations are presented mainly to support the interpretation of the results. They are not a complete theory in that they do not predict the initial wave that appears nor do they take account of viscous damping.

Discussion of Results for $u_{SG} > 3$ m/s

The final stage in slug formation described previously is a nonlinear Kelvin-Helmholtz instability, in that the wave has to reach a certain height before the destabilizing effects of gas-phase pressure variations dominate. For large u_{SG} (say $u_{SG} >$ about 4 m/s), the stratified flow shows a linear Kelvin-Helmholtz instability. The properties of the waves formed by this instability on thin liquid layers have already been carefully documented by Andritsos and Hanratty (1987a), who showed that they are associated with large increases in the interfacial stress. Similar wave structures were observed in this study, for $u_{SG} = 4$ m/s and $u_{SG} = 6$ m/s at liquid heights close to what is required for the initiation of slugging.

It is noted in both of these experiments (Figures 12 and 13) that, at a short distance (for example, $L = 7.02$ m) from the entry, the wave spectra are characterized by a peak with a dimensionless frequency of 0.2 and a median dimensionless frequency of 0.35 to 0.45. Small-amplitude waves with this frequency would be outside the range where they would be destabilized by gas-phase pressure variations in phase with the wave height. Consequently, the picture presented is that capillary-gravity waves generated by a Kelvin Helmholtz instability rapidly evolve into long-wavelength waves that are not KH-unstable and that are sustained by energy fed by the gas. The triggering process by which these waves evolve into slugs is not completely understood.

Concluding Remarks

Scope

This article describes wave pattern changes along a horizontal 9.53-cm pipe through which air and water flow. The focus is to provide an understanding of how slugs evolve. The chief impacts are to predict the initiation of slugging and the frequency of slugging.

Four mechanisms have been identified for the initiation of slugging: (1) the direct growth of slugs on an interface, by a Kelvin-Helmholtz mechanism, from linearly unstable long-wavelength disturbances; (2) the evolution of slugs from finite-amplitude waves with wavelengths in a range that would be predicted to be stable by a linear Kelvin-Helmholtz analysis; (3) the evolution of slugs through the coalescence of waves; (4) the initiation of slugs through large hydrodynamic disturbances at the inlet. In addition, the flow must meet necessary conditions for the existence of stable slugs (Ruder et al., 1989). Any of these (and, perhaps, others still to be discovered) can provide the basis for predicting critical conditions. Because of this complexity and the limited range of variables studied, no attempt is made here to develop general stability correlations. Instead, the focus is on mechanism.

Initiation of slugs at $u_{SG} \leq 3$ m/s

At $u_{SG} \leq 3$ m/s, slugs appeared at values of $\bar{h}_L$ in agreement with the viscous long-wavelength linear Kelvin-Helmholtz stability analysis. Surprisingly, however, transition was observed to occur by a different mechanism than this analysis suggests. The slugs did not evolve directly from very long-wavelength waves. Rather, they evolved indirectly from short-wavelength gravity waves (approximately 8.5 cm). These waves double in wavelength as they propagate downstream. This result agrees with a theory by Chen and Saffman (1979, 1980) and is the first observation of bifurcation in pipeline flows. The growth in amplitude of $\lambda_1 \cong 8.5$ cm waves, as they propagate downstream, is accompanied by an increase in wave velocity. Eventually, these waves reach a velocity equal to that for a small-amplitude $\lambda_2 = 2\lambda_1$ wave. This opens the possibility of a resonant interaction and a rapid transfer of energy from the λ_1 wave to a $\lambda_2 = 2\lambda_1$ wave. At small $\bar{h}_L$, the λ_2 waves can decay or they can grow until they reach a maximum height at which they tumble. At large enough $\bar{h}_L$, these waves can grow to large

enough heights (before they tumble) so that a nonlinear Kelvin-Helmholtz instability is possible. This leads to the formation of a slug that will grow if the liquid layer in front of the slug exceeds that defined by the necessary conditions for the existence of a slug.

The same phenomena and the same unstable wavelengths (8.5 and 17 cm) were also observed for $u_{SG}=1$, 2 and 3 m/s. This suggests a characteristic length and velocity for these experiments of D and $(gD)^{1/2}$.

An analysis of the initiation of slugs by the process will need to predict the initial wave that appears close to the inlet and whether the liquid height is large enough for this wave to evolve into a slug. The initial waves (at $u_{SG} \leq 3$ m/s) are generated by a Jeffreys mechanism (Hanratty, 1983, 1991) whereby gas-phase pressure variations in phase with the wave slope feed energy to a wave at a rate which exceeds viscous dissipation. A plausible assumption is that the observed dominant wave is the fastest growing wave. A study of Jeffrey waves in confined spaces has been presented by Cohen and Hanratty (1965). They show that the appearance of very long-wavelength waves is not possible because of strong viscous dissipation of boundary layers at the wall and that the appearance of very short-wavelength waves is inhibited by a viscous boundary layer at the interface. As a consequence, the wavelength, λ_1, of the fastest growing wave scales with $\bar{h}_L$ (from Cohen and Hanratty roughly $\lambda \approx 2\bar{h}_L$). These λ_1 waves can grow until they saturate, by tumbling and by passing energy to waves with other harmonics, or they strike the top wall. The calculation of the correct outcome requires a complicated nonlinear analysis, which needs experimental guidance.

This study shows, for conditions close to those required for initiation of slugs, that the λ_1 waves double in wavelength and that the nonlinear analysis ought to focus on the waves that result from this bifurcation. These λ_2 waves receive energy from the λ_1 waves and directly from the air flow through the Jeffreys mechanism. The λ_2 waves can be more dissipative than the λ_1 waves, since $\lambda/\bar{h}_L$ is twice as large. Consequently, a first consideration is whether λ_2 waves can be sustained completely by energy fed from the gas flow.

If this is the case, then the very rough calculations could present some guidelines. These use the suggestion by Banner and Phillips that waves reach a limiting height when the liquid velocity at the interface becomes equal to the wave velocity. They produce the interesting result that $(C-\bar{u}_L)$ needs to be below a certain value for the wave to reach a limiting height. For small $\bar{h}_L/D$, this criterion is satisfied. However, if $\bar{h}_L/D$ is large enough, $(c-\bar{u}_L)$ will have values such that a growing wave never reaches a limiting height. The final outcome for these latter waves is that the gas velocity at the crest reaches high enough values that a Bernoulli effect causes the wave to strike the top wall.

Initiation of slugs at $u_{SG} > 4$ m/s

An analysis of the evolution of slugs for $u_{SG} > 4$ m/s appears more difficult than that for lower gas velocities. As already pointed out, small-wavelength capillary-gravity waves formed at the inlet rapidly evolve into longer-wavelength irregular waves that have reached their limiting height.

It seems plausible that for very high $\bar{h}_L/D$, these gravity waves could grow until they reach the top wall, as is suggested by the experiments by Andritsos et al. for low air flows over viscous liquids. This is not the case for low $\bar{h}_L/D$, where the waves are observed to reach a limiting height. Consequently, it is surprising that slugs can be formed under such conditions.

These irregular waves, however, have a range of velocities so that they can overtake one another. Lin and Hanratty (1986, 1987a), Andritsos et al. (1989), and this study all show that this coalescence of waves can precipitate the formation of slugs at some critical $\bar{h}_L/D$. In fact, this seems to be the dominant mechanism for viscous liquids at low $\bar{h}_L/D$ and for water at high gas velocities.

A theoretical basis for predicting this critical $\bar{h}_L/D$ is not known. One possibility is that the coalescence creates larger-amplitude waves with a larger velocity; this wave could reach the top wall by a process similar to that described for the λ_2 waves at $u_{SG} < 3$ m/s. However, an important consideration is whether the environment around this coalesced wave satisfies conditions necessary to sustain a slug.

Frequency of slugging

If the liquid flow rate and the pipe length are large enough that several slugs exist in the pipeline at any time, the processes described for the initiation of slugging move closer to the inlet.

The formation of a slug under these conditions is followed by a drop of the liquid level. Another stable slug cannot form until the liquid level builds up to a sufficient height for the initiation process to occur and for the slug to maintain itself as it propagates downstream. The latter height is dictated by necessary conditions for the existence of slugs (Ruder et al., 1989) and is smaller than the height required to initiate slugs. The prediction of liquid buildup is complicated, because it occurs by the propagation of large-amplitude waves and unstable slugs, as well as by hydraulic gradients. Other complications are the possibility of the continuous decay and formation of slugs throughout a pipeline, particularly at $u_{SG} \geq 4$ m/s, and the uncertainty regarding the role of pressure (or flow) pulsations caused by the discharge of a slug from the outlet of the pipe.

It is clear that any analysis which uses insights from the mechanism of slug formation to predict slug frequency must be accompanied by careful and detailed experimentation. Nevertheless, our results can be used to evaluate analyses presently available in the literature. Taitel and Dukler (1977) explored the notion that slug frequency is determined by the time for the liquid at the inlet to build up from the level required to initiate slugs (Figure 6) to the equilibrium level that would exist for a stratified flow at the prevailing gas and liquid flow rates. Our study suggests that a better choice would be a buildup from a very small liquid level to the level required to initiate slugs. Likewise, the suggestion by Traconic (1990) that the slug frequency is one-half the frequency of unstable waves does not seem consistent with our results.

Acknowledgment

This work has been supported by the Department of Energy under DOE DEF GO2-86ER13556.

Literature Cited

Andritsos, N., "Effect of Pipe Diameter and Liquid Viscosity on

Horizontal Stratified Flow," PhD Thesis, Univ. of Illinois, Urbana (1986).
Andritsos, N., and T. J. Hanratty, "Interfacial Instabilities for Horizontal Gas-Liquid Flows in Pipelines," *Int. J. Multiphase Flow*, **13**, 583 (1987a).
Andritsos, N., and T. J. Hanratty, "Influence of Interfacial Waves in Stratified Gas-Liquid Flows," *AIChE J.*, **33**, 444 (1987b).
Andritsos, N., L. Williams, and T. J. Hanratty, "Effect of Liquid Viscosity on the Stratified-Slug Transition in Horizontal Pipe Flow," *Int. J. Multiphase Flow*, **15**, 877 (1989).
Andritsos, N., V. Bontozoglou, and T. J. Hanratty, "Transition to Slug Flow in Horizontal Pipes," *Chem. Eng. Comm.*, **118**, 361 (1992).
Bahner, M. L., and W. K. Meville, "On the Separation of Air Flow over Water Waves," *J. Fluid Mech.*, **77**, 825 (1976).
Banner, M. L., and O. M. Phillips, "On the Incipient Breaking of Small Scale Waves," *J. Fluid Mech.*, **65**, 647 (1974).
Bontozoglou, V., and T. J. Hanratty, "Effects of Finite Depth and Current Velocity on Large Amplitude Kelvin-Helmholtz Waves," *J. Fluid Mech.*, **196**, 187 (1988).
Bontozoglou, V., and T. J. Hanratty, "Capillary-Gravity Kelvin-Helmholtz Waves Close to Resonance," *J. Fluid Mech.*, **217**, 71 (1990).
Chen, B., and P. G. Saffman, "Steady Gravity-Capillary Waves on Deep Water: I. Weakly Nonlinear Waves," *Stud. Appl. Math.*, **60**, 183 (1979).
Chen, B., and P. G. Saffman, "Steady Gravity-Capillary Waves on Deep Water: II. Numerical Results for Finite Amplitude," *Stud. Appl. Math.*, **62**, 95 (1980).
Cohen, L. S., and T. J. Hanratty, "Generation of Waves in the Concurrent Flow of Air and a Liquid," *AIChE J.*, **11**, 138 (1965).
Hanratty, T. J., "Interfacial Instabilities Caused by the Air Flow over a Thin Liquid Layer," *Waves on Fluid Interfaces*, R. E. Meyer, ed., p. 221, Academic Press, New York (1983).
Hanratty, T. J., and J. M. Engen, "Interaction between a Turbulent Air Stream and a Moving Water Surface," *AIChE J.*, **3**, 299 (1957).
Hanratty, T. J., "Separated Flow Modelling and Interfacial Transport Phenomena," *Appl. Sci. Res.*, **48**, 353 (1991).
Hwang, P. A., D. Xu, and J. Wu, "Breaking of Wind-Generated Waves: Measurements and Characteristics," *J. Fluid Mech.*, **202**, 177 (1989).
Kordyban, E. S., and T. Ranov, "Mechanism of Slug Formation in Horizontal Two-Phase Flow," *J. Basic Eng.*, **92**, 857 (1970).
Kordyban, E., "The Transition to Slug Flow in the Presence of Large Waves," *Int. J. Multiphase Flow*, **3**, 603 (1977).
Lamb, H., *Hydrodynamics*, Cambridge University Press, p. 420 (1953).
Lin, P. Y., and T. J. Hanratty, "Prediction of the Initiation of Slugs with Linear Stability Theory," *Int. J. Multiphase Flow*, **12**, 79 (1986).
Lin, P. Y., and T. J. Hanratty, "Effect of Pipe Diameter on Flow Patterns for Air-Water Flow in Horizontal," *Int. J. Multiphase Flow*, **13**, 549 (1987a).
Lin, P. Y., and T. J. Hanratty, "Detection of Slug Flow from Pressure Measurements," *Int. J. Multiphase Flow*, **13**, 13 (1987).
Minato, A., T. Ikeda, and M. Naitoh, "Mechanistic Model of Slugging Onset in Horizontal Circular Tubes," *J. Nucl. Sci. and Technol.*, **23**, 761 (1986).
Mishima, K., and M. Ishii, "Theoretical Prediction of Onset of Horizontal Slug Flow," *J. Fluids Eng., ASME Trans.*, **102**, 441 (1980).
Phillips, O. M., and M. L. Banner, "Wave Breaking in the Presence of Wind Drift and Swell," *J. Fluid Mech.*, **66**, 625 (1974).
Ruder, Z., P. J. Hanratty, and T. J. Hanratty, "Necessary Conditions for the Existence of Slugs," *Int. J. Multiphase Flow*, **15**, 135 (1989).
Taitel, Y., and A. E. Dukler, "A Model for Predicting Flow Regime Transition in Horizontal and Near Horizontal Gas-Liquid Flow," *AIChE J.*, **22**, 47 (1976).
Taitel, Y., and A. E. Dukler, "A Model for Slug Frequency in Horizontal and Near Horizontal Pipes," *Int. J. Multiphase Flow*, **3**, 585 (1977).
Tronconic, E., "Prediction of Slug Frequency in Horizontal Two-Phase Slug Flow," *AIChE J.*, **36**, 701 (1990).
Wallis, G. B., and J. E. Dobson, "The Onset of Slugging in Horizontal Stratified Air-Water Flow," *Int. J. Multiphase Flow*, **1**, 173 (1973).
Williams, L. R., "Effect of Pipe Diameter on Horizontal Annular Two-Phase Flow," PhD Thesis, Chemical Engineering Dept., Univ. of Illinois, Urbana (1990).
Wu, H. L., B. F. M. Pots, J. F. Holenburg, and Meerhoff, "Flow Pattern Transition in Two-Phase Gas/Condensate Flow at High Pressure in an 8-in. Horizontal Pipe," BHRA Conf., The Hague (May 18-26, 1987).

Manuscript received Apr. 17, 1992, and revision received Feb. 3, 1993.